TWMS J. App. and Eng. Math. V.11, N.1, 2021, pp. 203-215

RBF SOLUTION OF MHD STOKES FLOW AND MHD FLOW IN A CONSTRICTED ENCLOSURE

MERVE GÜRBÜZ[1], M. TEZER-SEZGIN[2], §

ABSTRACT. This paper presents the radial basis function (RBF) approximation for the numerical solution of Stokes and Navier-Stokes equations in a constricted enclosure under the effect of magnetic field with different orientations. RBFs are used for the approximation of the particular solution which becomes also the approximate solution of the problem satisfying the boundary conditions. Numerical results are obtained for several values of Hartmann number and constriction ratio. As the strength of the horizontally applied magnetic field increases, Stokes flow extends covering the whole pipe. Applied magnetic field in the pipe-axis direction generates the electric potential exhibiting behavior similar to streamlines. When the constriction ratio increases, flow squeezes through the left wall regardless of the direction of the magnetic field.

Keywords: MHD, Stokes flow, RBF, electric potential, constricted pipe.

AMS Subject Classification: 65N35, 76D07, 76W05

1. Introduction

Magnetohydrodynamic (MHD) is the field which deals with the interaction between electrically conducting fluids and magnetic fields. It has a widespread applications in science and technology such as MHD generators, electromagnetic pumps, cooling system with liquid metals for nuclear reactors, plasma physics, blood flow measurement, etc. The MHD equations are governed by the Navier-Stokes equations of fluid dynamics and Maxwell's equations of electromagnetics through the Ohm's law.

The incompressible, viscous flow in slow motion is called Stokes flow (or creeping flow) which has many industrial applications such as hydrodynamic lubrication, food-processing materials, etc. Stokes flow equations are obtained from the momentum equations neglecting the convection terms due to the small values of Reynolds number ($Re << 1$). Eldho and Young [3] considered Stokes flow in a lid-driven cavity. They obtained the numerical results for $Re = 0$ and $Re = 1$ by using dual reciprocity boundary element method

[1] Başkent University, Faculty of Economics and Administrative Sciences, Department of Management, Ankara, Turkey.
e-mail: mervegurbuz@baskent.edu.tr; ORCID: https://orcid.org/0000-0002-7746-9005.
[2] Middle East Technical University, Faculty of Arts and Sciences, Department of Mathematics, Ankara, Turkey.
e-mail: munt@metu.edu.tr; ORCID: https://orcid.org/0000-0001-5439-3477.
§ Manuscript received: March 13, 2019; accepted: May 18, 2019.

(DRBEM). The behavior of the Stokes flow in square and circular cavities was analyzed by Young et al. [17]. They used DRBEM based on compactly-supported, positive-definite radial basis functions to solve the equations in the stream function-vorticity formulation. In another study of Young et al. [15], method of fundamental solution (MFS) was applied to the Stokes flow in a lid-driven cavity with wavy bottom and in a cubic cavity. They showed the effect of source points and their locations on the accuracy of numerical results. Kolodziej and Grabski [7] considered the viscous, laminar flow in a wavy channel. They also simulated the flow behavior taking $Re = 0$ by using MFS and RBF. Vasudeviah and Balamurugan [13] solved stream function and temperature equations of forced convection Stokes flow in a wavy channel. In [4], biharmonic form of the Stokes equation was solved by the method of superposition to study distributive mixing produced by rotating cylinder in the center of the cavity. Stokes flow equations have been also solved by using RBF approximation in [16, 1, 8]. In all of these studies, multiquadratic (MQ) RBF is used to solve Stokes flow in cavities and in a backward-facing step channel. The magnetic field effect on the Stokes flow past circular cylinder was added by Yosinobu and Kakutani [14]. Gürbüz and Tezer-Sezgin [5] implemented RBF approximation to obtain the numerical solution of the slow flow in a lid-driven cavity and in a backward-facing step channel under the uniform magnetic field with different orientations. The electric potential for the Stokes flow in the lid-driven cavity was also simulated when the magnetic field is parallel to the pipe-axis. MHD equations coupled with energy equation are considered in [11, 12].

In the present study, the MHD Stokes flow and MHD incompressible flow are considered in a constricted enclosure (cross-section of the pipe) with a moving left wall. External magnetic field is applied from the $x-$, $y-$ or $z-$directions. RBF approximation has been applied for solving the MHD flow equations in terms of the original variables as the velocity components of the fluid, stream function, vorticity, pressure of the fluid and the electric potential with a considerably low computational expense. The main aim of this study is to show the effects of both the magnetic field and the constriction ratio on the Stokes and incompressible flows. The computations are carried out for the several values of Hartmann number and constriction ratio. As the horizontally applied magnetic field intensity increases in the Stokes flow, fluid flows in the whole channel. On the other hand, the effects of the vertical magnetic field and the moving left wall force the fluid to concentrate through the left wall. When the enclosure is constricted, the magnitude of the flow decreases regardless of the direction of the magnetic field. The secondary flow is observed due to the constriction in the case of vertically applied magnetic field. Fluid moves through the left wall with a further increase in the constriction ratio [6]. Additionally, MHD flow with a magnetic field in the pipe-axis direction is simulated exhibiting the electric potential. The effects of magnetic field and constriction ratio on the electric potential are also analyzed. The constriction effect on the flow is the same as in the case of the vertically applied magnetic field.

2. Physical problem and mathematical formulation

The steady, laminar fully-developed flow of an incompressible, viscous, electrically conducting fluid in the cross-section (enclosure) of a long pipe is considered. A uniform magnetic field is applied in the horizontal, vertical or along the pipe-axis directions. The left wall of the enclosure is moving upwards with a uniform velocity. Figure 1 displays the problem configuration.

The middle section of the enclosure is symmetrically constricted using functions f_b and f_t. These functions are defined as $f_b = \frac{1}{2}h(1+\cos(2\pi(x-\frac{1}{2})))$, $f_t = 1 - f_b$ and the constriction ratio(CR) of the enclosure is defined as $CR = 2h \times 100$.

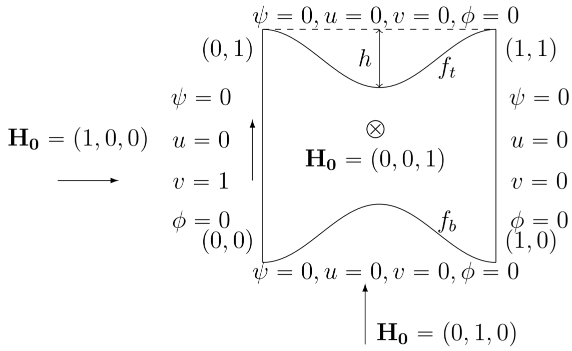

FIGURE 1. Problem configuration

The non-dimensional MHD equations [14, 9] are given as

$$\nabla \cdot \mathbf{u} = 0 \tag{1}$$

$$Re(\mathbf{u}\cdot\nabla)\mathbf{u} = -\nabla p + \nabla^2\mathbf{u} + M^2(-\nabla\phi + \mathbf{u}\times\mathbf{H})\times\mathbf{H} \tag{2}$$

$$Re_m(-\nabla\phi + \mathbf{u}\times\mathbf{H}) = \nabla\times\mathbf{H} \tag{3}$$

where $\mathbf{u} = (u, v, 0)$, $\mathbf{H} = (H_x, H_y, H_z)$, p, $\mathbf{J}$ and ϕ are the fluid velocity, magnetic field, pressure of the fluid, electric current density and electric potential, respectively. The non-dimensional parameters are the Reynolds number $Re = LU_0/\nu$, the magnetic Reynolds number $Re_m = LU_0\sigma\mu$ and the Hartmann number $M = L\mu H_0\sqrt{\sigma/\rho\nu}$. Here, ρ, ν, μ and σ are the density, the kinematic viscosity, the magnetic permeability and the electric conductivity of the fluid. The last term in equation (2) is the Lorentz force coming from the interaction between the electrically conducting fluid and the external magnetic field. Induced magnetic field is neglected in the equation (3) due to the low magnetic Reynolds number $Re_m << 1$. Thus, equation (3) is no more used in the solution procedure.

2.1. **MHD Stokes flow.** Stokes flow approximation considers very small values of Reynolds number ($Re << 1$) so that the convective terms in the equation (2) are neglected. Hence, the MHD Stokes flow equations in terms of primitive variables, the velocity and pressure are

$$\nabla \cdot \mathbf{u} = 0 \tag{4}$$

$$-\nabla p + \nabla^2\mathbf{u} + M^2(-\nabla\phi\times\mathbf{H} + \mathbf{u}\times\mathbf{H}\times\mathbf{H}) = 0 \ . \tag{5}$$

When the magnetic field is applied horizontally or vertically, we obtain $\nabla^2\phi = 0$ from Ohm's law $\mathbf{J} = \sigma(-\nabla\phi + \mathbf{u}\times\mu\mathbf{H})$ and Ampere law $\mathbf{J} = \nabla\times\mathbf{H}$. With the homogeneous boundary conditions the solution becomes the zero electric potential, $\phi = 0$, dropping the gradient of the electric potential in the equation (5), ($\nabla\phi = 0$).

When the magnetic field applies in the $x-$direction, $\mathbf{H_0} = (1, 0, 0)$, the equations take the form

$$\frac{\partial u}{\partial x} + \frac{\partial v}{\partial y} = 0, \quad \nabla^2 u = \frac{\partial p}{\partial x}, \quad \nabla^2 v = \frac{\partial p}{\partial y} + M^2 v. \tag{6}$$

In the cross-section of the pipe, the two-dimensional flow allows one to define the stream function ψ and the vorticity ω as

$$u = \frac{\partial \psi}{\partial y}, \quad v = -\frac{\partial \psi}{\partial x}, \quad \omega = \frac{\partial v}{\partial x} - \frac{\partial u}{\partial y}. \tag{7}$$

Then, the two-dimensional MHD Stokes flow equations are given for all of the problem variables u, v, ψ, ω, and p

$$\nabla^2 u = -\frac{\partial \omega}{\partial y}, \qquad \nabla^2 v = \frac{\partial \omega}{\partial x}, \qquad \nabla^2 \psi = -\omega \tag{8}$$

$$\nabla^2 \omega = M^2 \frac{\partial v}{\partial x}, \qquad \nabla^2 p = -M^2 \frac{\partial v}{\partial y} \quad . \tag{9}$$

When the magnetic field is acted vertically, $\mathbf{H_0} = (0, 1, 0)$, the equation (5) converts to

$$\nabla^2 u = \frac{\partial p}{\partial x} + M^2 u, \quad \nabla^2 v = \frac{\partial p}{\partial y} \tag{10}$$

which can be also written in terms of all the fluid variables

$$\nabla^2 u = -\frac{\partial \omega}{\partial y}, \qquad \nabla^2 v = \frac{\partial \omega}{\partial x}, \qquad \nabla^2 \psi = -\omega \tag{11}$$

$$\nabla^2 \omega = -M^2 \frac{\partial u}{\partial y}, \qquad \nabla^2 p = -M^2 \frac{\partial u}{\partial x} \quad . \tag{12}$$

2.2. **Incompressible MHD flow.** The electric potential can be generated in the two-dimensional cross-section of a pipe (enclosure) only when the external magnetic field applies along the pipe-axis direction. Then, the equation (2) can be written component-wise

$$\frac{1}{N}(u\frac{\partial u}{\partial x} + v\frac{\partial u}{\partial y}) = -\frac{1}{M^2}\frac{\partial p}{\partial x} + \frac{1}{M^2}\nabla^2 u + \left(-u - \frac{\partial \phi}{\partial y}\right) \tag{13}$$

$$\frac{1}{N}(u\frac{\partial v}{\partial x} + v\frac{\partial v}{\partial y}) = -\frac{1}{M^2}\frac{\partial p}{\partial y} + \frac{1}{M^2}\nabla^2 v + \left(-v + \frac{\partial \phi}{\partial x}\right) \tag{14}$$

where N is the Stuart number given by $N = M^2/Re$. Using the vorticity definition, and Ohm's law and Ampere law, we obtain the electric potential Poisson's equation $\nabla^2 \phi = \omega$. Thus, the MHD flow together with an electric potential is governed by the equations

$$\nabla^2 u = -\frac{\partial \omega}{\partial y}, \qquad \nabla^2 v = \frac{\partial \omega}{\partial x}, \qquad \nabla^2 \psi = -\omega, \qquad \nabla^2 \phi = \omega \tag{15}$$

$$\frac{1}{M^2}\nabla^2 \omega = \frac{1}{N}\left(u\frac{\partial \omega}{\partial x} + v\frac{\partial \omega}{\partial y}\right), \quad \frac{1}{M^2}\nabla^2 p = \frac{2}{N}\left(\frac{\partial u}{\partial x}\frac{\partial v}{\partial y} - \frac{\partial u}{\partial y}\frac{\partial v}{\partial x}\right) \tag{16}$$

under the effect of a magnetic field perpendicular to the enclosure.

The boundary conditions for the velocity, stream function and the electric potential are shown in the Figure 1. The unknown boundary conditions for the vorticity are obtained from the finite difference approximation of the stream function equation including interior values of stream function. Pressure boundary values are computed by using the finite difference scheme for the gradient of pressure and the coordinate matrix for the space derivatives in the momentum equations.

3. RBF approximation

The radial basis function approximation will be shortly described on a boundary value problem

$$Lu(x,y) = f(x,y), \qquad (x,y) \in \Omega \tag{17}$$

$$Bu(x,y) = g(x,y), \qquad (x,y) \in \partial\Omega \tag{18}$$

where L and B are linear partial differential and boundary operators, respectively, f and g are known functions in the domain Ω with the boundary $\partial\Omega$.
In the radial basis function approximation method [2], both $f(x,y)$ and the particular solution $\hat{u}$ are written in terms of a finite series of radial basis functions $\{\varphi_j\}$ and $\{\psi_j\}$ as

$$f(x,y) = \sum_{j=1}^{n} a_j \varphi_j(r), \quad \hat{u}(x,y) = \sum_{j=1}^{n} a_j \Psi_j(r) \qquad (x,y) \in \Omega \tag{19}$$

where $r = ((x-x_j)^2 + (y-y_j)^2)^{1/2}$ is the Euclidean distance and n is the number of unknown coefficients. ψ_j's are linked through $L\Psi_j(r) = \varphi_j(r)$. $\hat{u}$ is forced to satisfy the boundary condition (18) as

$$\sum_{j=1}^{n} a_j B\Psi_j(r) = g(x,y), \qquad (x,y) \in \partial\Omega \ . \tag{20}$$

Since $\hat{u}$ satisfies both the differential equation and the boundary condition, it becomes the approximate solution of the equation (17). The coefficients a_j in the approximation (19) are determined by taking $N_b + N_i = n$ collocation points (x_i, y_i) on the boundary and interior of the domain, and solving the two linear systems

$$\sum_{j=1}^{n} a_j B\Psi_j(r_k) = g(x_k, y_k), \quad 1 \le k \le N_b \quad \text{and} \quad \sum_{j=1}^{n} a_j \varphi_j(r_l) = f(x_l, y_l), \quad 1 + N_b \le l \le n \tag{21}$$

which are combined to give one linear system $[A]\{a\} = \{b\}$ for the solution vector $\{a\} = \begin{bmatrix} a_1 & \cdots & a_n \end{bmatrix}^t$. The coefficient matrix and the right hand side vector are given as

$$[A] = \begin{bmatrix} B\Psi_1(r_1) & B\Psi_2(r_1) & \cdots & B\Psi_n(r_1) \\ \vdots & \vdots & \ddots & \vdots \\ B\Psi_1(r_{N_b}) & B\Psi_2(r_{N_b}) & \cdots & B\Psi_n(r_{N_b}) \\ \varphi_1(r_{N_b+1}) & \varphi_2(r_{N_b+1}) & \cdots & \varphi_n(r_{N_b+1}) \\ \vdots & \vdots & \ddots & \vdots \\ \varphi_1(r_n) & \varphi_2(r_n) & \cdots & \varphi_n(r_n) \end{bmatrix}_{n\times n}, \ \{b\} = \begin{bmatrix} g(x_1, y_1) \\ \vdots \\ g(x_{N_b}, y_{N_b}) \\ f(x_{N_b+1}, y_{N_b+1}) \\ \vdots \\ f(x_n, y_n) \end{bmatrix}_{n\times 1}.$$

The solution of the system gives the coefficients a_j, $1 \le j \le n$ and then the approximate solution becomes $\hat{u}(x,y) = \sum_{j=1}^{n} a_j \Psi_j(r)$.

In this study, all of the equations (8)-(9), (11)-(12) and (15)-(16) are Poisson's type equations, and they are solved iteratively by using RBF approximation. That is, $L = \nabla^2$, the Laplace operator and $B = I$, the identity boundary operator for all of the equations. We have used linear, quadratic polynomials and multiquadratic RBFs which resulted in insignificant differences in the flow behavior. Thus, the computations are carried with linear RBF for the computational simplicity as $\varphi(r) = 1 + r$ giving $\Psi(r) = \dfrac{r^2}{4} + \dfrac{r^3}{9}$. The iterative process starts with an initial estimate of the vorticity and solving the equations in the order for the velocity components, stream function, vorticity and pressure. The electric potential is obtained when the velocity components are available from the equations (15). The iteration continues until a preassigned tolerance (ϵ) is reached between two successive iterations by using maximum absolute error. In each iteration, all the required space derivatives of the unknowns are obtained with the use of coordinate matrix φ as $\dfrac{\partial D}{\partial x} = \dfrac{\partial \varphi}{\partial x}\varphi^{-1}D$, $\dfrac{\partial D}{\partial y} = \dfrac{\partial \varphi}{\partial y}\varphi^{-1}D$ where D denotes u, v and ω.

4. Numerical results

The steady MHD Stokes and incompressible MHD flows in a constricted enclosure with a moving left wall are analyzed by using RBF approximation. External magnetic field applies in the $x-$, $y-$ or $z-$directions. We take stopping criteria tolerance for the pressure as 10^{-3} using maximum absolute error. Relaxation parameters α and β, $0 \leq \alpha, \beta \leq 1$ for the vorticity and pressure values are used to accelerate the convergence. We discretize the boundary of the enclosure by taking $N_b = 96$ and $N_b = 120$ uniformly distributed points for the MHD Stokes flow and the MHD flow, respectively. The system of equations for u, v, ψ and p are solved using 'mldivide' function in MATLAB.

4.1. **Magnetic field in the $x-$direction.** The two-dimensional MHD Stokes flow equations (8)-(9) are solved iteratively when the magnetic field is acted horizontally. To see the effects of both magnetic field and the constriction of the pipe on the Stokes flow we take several values of Hartmann number ($0 \leq M \leq 100$) and the constriction ratio of the enclosure ($0\% \leq CR \leq 75\%$). The numerical solution is shown in terms of stream function, vorticity and pressure in Figures 2-4.

Figure 2 shows the effect of magnetic field on the Stokes flow in a non-constricted enclosure. In the absence of the magnetic field ($M = 0$), Stokes flow is concentrated in front of the left moving wall with a similar profile in a cavity with moving top lid as given in [15]. As the intensity of the magnetic field increases, fluid flows in almost all parts of the enclosure. Also, the main vortex of the flow shifts through the center of the enclosure. Further increase in M causes side layers to be formed on the walls parallel to the applied magnetic field and also Hartmann layers on the vertical walls especially pronounced on the left wall with the effect of its movement upwards. The vorticity has the expected behavior due to the movement of the left wall when M is small. But, it forms the boundary layers leaving the central part almost stagnant as M increases. Pressure is uniformly distributed with an increasing value between the top and the bottom walls as M increases.

In Figure 3, we fix the constriction ratio to $CR = 25\%$ and increase Hartmann number to analyze the impact of the magnetic field on the Stokes flow in a constricted enclosure. When the pipe is constricted, pressure tends to be increased at the right corners, the behavior of the flow does not change significantly, but the flow is mostly concentrated near the left moving wall and in the constricted area leaving the parts close to the right corners stagnant. Horizontally applied magnetic field with an increasing intensity retards the effect of moving left wall as in the case of non-constricted cavity (Figure 2) extending the flow to the whole enclosure.

The effect of the constriction ratio on the MHD Stokes flow under the effect of horizontal magnetic field is depicted in Figure 4. When the constriction is further increased, the fluid completely flows in the left constricted part and the rest of the cavity is stagnant. Constriction deteriorates the uniform distribution of pressure. Pressure contours are anti-symmetrically squeezed through the corners of the cavity with respect to $y = 0.5$ line.

4.2. **Magnetic field in the $y-$direction.** With a uniform magnetic field applied in the $y-$direction, MHD Stokes flow equations (11)-(12) are solved for several Hartmann number values ($0 \leq M \leq 100$) and constriction ratios ($0\% \leq CR \leq 75\%$). The flow characteristics are shown in Figures 5-7.

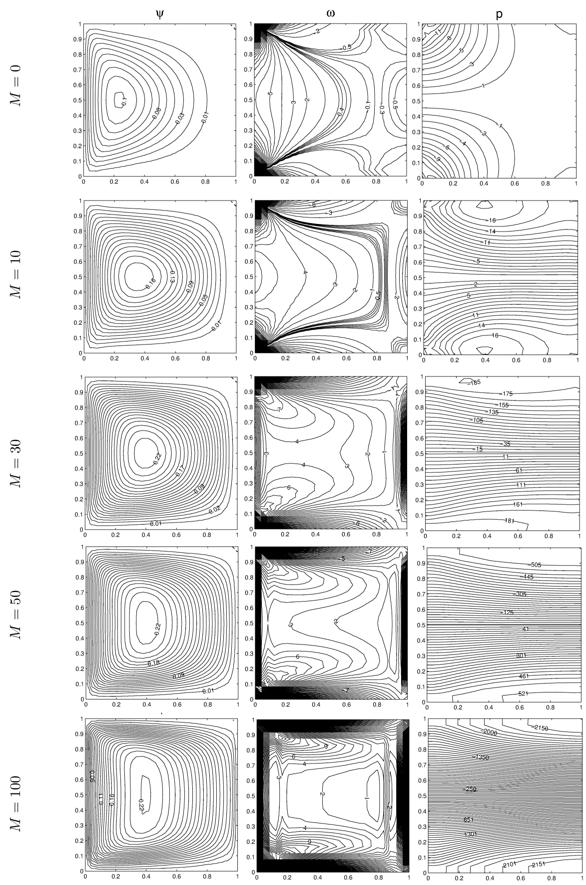

FIGURE 2. MHD Stokes flow with $CR = 0\%$, $\mathbf{H_0} = (1, 0, 0)$.

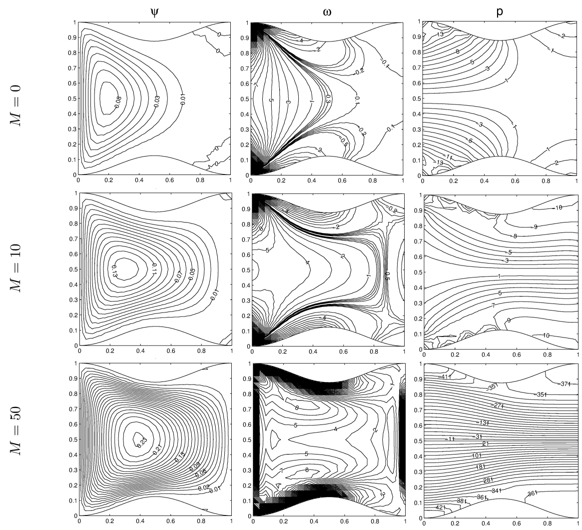

FIGURE 3. MHD Stokes flow with $CR = 25\%$, $\mathbf{H_0} = (1, 0, 0)$.

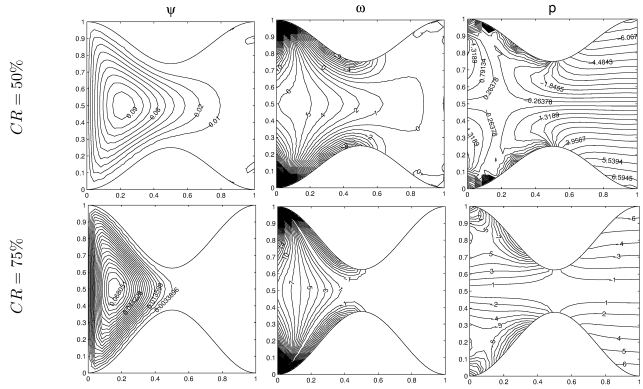

FIGURE 4. MHD Stokes flow with $M = 10$, $\mathbf{H_0} = (1, 0, 0)$.

The influence of the vertical magnetic field on the creeping flow in an enclosure with a moving left lid is shown in Figure 5. The behaviors of the flow and pressure are completely different from the ones obtained with horizontally applied magnetic field which can be seen by comparing the results given in Figure 2 and Figure 5. As M increases, the flow is retarded and completely concentrated through the moving left wall forming boundary side layer. This is due to the direction of magnetic field which is the same with the moving left wall. Further increase in M, secondary flow with a small magnitude occurs and the rest of the cavity is stagnant. As the strength of the vertical magnetic field increases, pressure is distributed anti-symmetrically with respect to horizontal centerline of the enclosure in terms of two loops mostly concentrated near the left wall.

Constricted enclosure with the ratio $CR = 25\%$ causes secondary flow and pressure appearance near the right corners when the magnetic field effect is absent. As M increases, secondary flow near the right wall enlarges first due to the constriction, but a further increase in M again pushes the flow through the moving left wall contrary to the effect of horizontally applied magnetic field (Figure 6). It was observed in Figure 3 that magnetic field acted in the $x-$direction retards the effect of moving lid and pushes the fluid to flow in the whole enclosure.

In Figure 7, we see the influence of further constrictions of the enclosure on the MHD Stokes flow. Secondary flow in front of the right wall enlarges first when the enclosure is constricted. Then, the effects of 75% constriction and moving left wall weaken this secondary flow and move the fluid through the left wall. The vorticity and pressure concentrate in front of the left moving lid as in the case of magnetic field acted in $x-$direction (Figure 4). Pressure appears at the right corners with an increasing value due to increase in the constriction showing the anti-symmetric profile again with respect to $y = 0.5$.

4.3. **Magnetic field in the $z-$direction.** The viscous, electrically conducting, incompressible fluid is considered in a constricted pipe under the effect of a magnetic field. The external magnetic field is applied in the pipe-axis direction, generating also the electric potential. Thus, the MHD equations (15)-(16) adopting electric potential are solved iteratively by taking several values of Hartmann number and the constriction ratios. We fix first the Stuart number as $N = 16$ and take Hartmann number values $M = 20$ and 40 which correspond to Reynolds numbers $Re = 25$ and 100, respectively, since $Re = M^2/N$ [10]. From the obtained numerical results, the flow, electric potential and pressure are simulated in Figures 8-10.

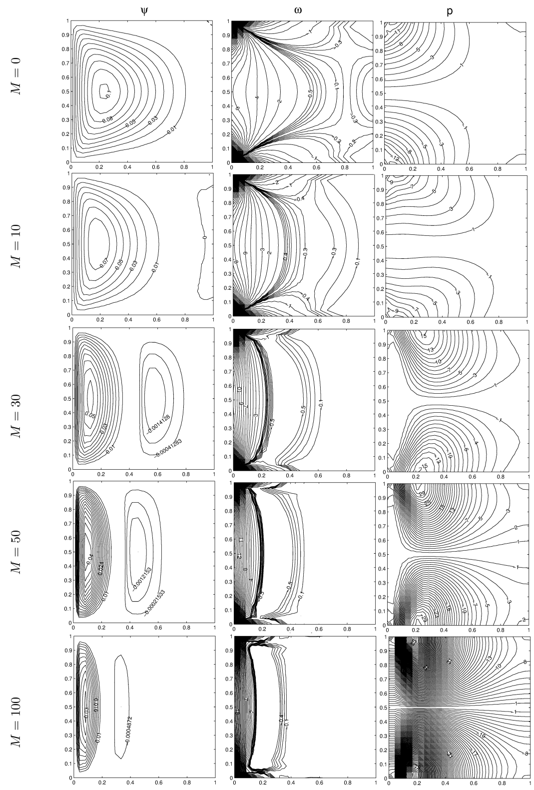

FIGURE 5. MHD Stokes flow with $CR = 0\%$, $\mathbf{H_0} = (0, 1, 0)$.

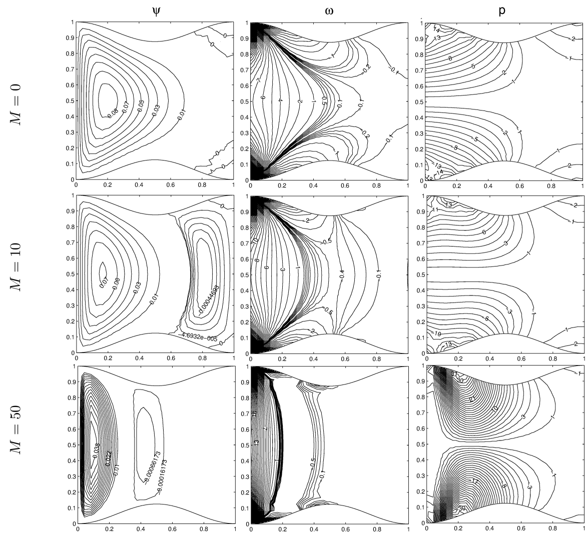

Figure 6. MHD Stokes flow with $CR = 25\%$, $\mathbf{H_0} = (0, 1, 0)$.

In Figure 8, the effect of perpendicularly applied magnetic field on the flow is analyzed in a non-constricted enclosure. As Hartmann number increases, streamlines and equivorticity lines move through the moving left wall forming boundary layer and the rest of the cavity is stagnant as in the case of $y-$direction magnetic field. The electric potential has the same behavior and magnitude of stream function since $\nabla^2\psi = -\omega$, $\nabla^2\phi = \omega$ and both ψ and ϕ vanish on the boundary. Symmetry in the flow and pressure with respect to $y = 0.5$ line is destroyed. Especially vorticity shows a fluctuation through the top wall and upper left corner instead of forming boundary layer near the left wall. This behavior is the result of strong magnetic field applied perpendicular to the cross-section (enclosure) of the pipe. Increase in the strength of the magnetic field increases the pressure values, but decreases magnitudes of stream function and electric potential. Pressure is unevenly distributed in the enclosure and highly concentrated at the moving left corner of the cavity as M increases.

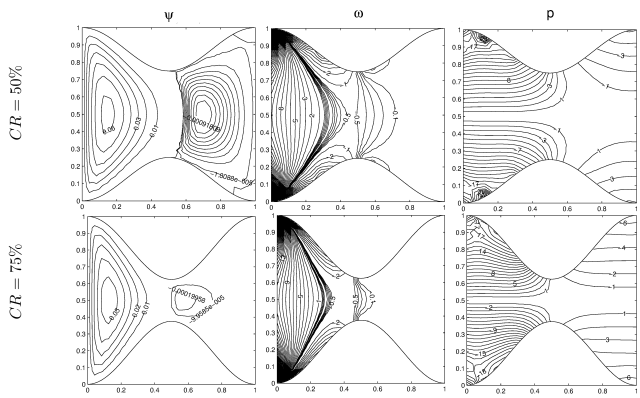

Figure 7. MHD Stokes flow with $M = 10$, $\mathbf{H_0} = (0, 1, 0)$.

Figures 9-10 show the effect of constriction on the incompressible MHD flow. It is observed that an increase in the constriction ratio of the enclosure leads to the development of secondary vortex in the right part of the enclosure for the flow and the electric potential. When the pipe is constricted further, this secondary vortex moves through the constricted area. Pressure is pronounced completely in the left part with descending values when the constriction of the enclosure is increased.

5. Conclusions

The RBF approximations to the MHD Stokes flow and MHD flow are given in a constricted square enclosure with a moving left wall. Flow is subjected to different orientations ($x-$, $y-$ or $z-$directions) of external magnetic field. We analyze the effects of both magnetic field and the constriction ratio on the MHD and MHD Stokes flows. For the Stokes flow an increase in the intensity of horizontal magnetic field overwhelms the effect of the moving left wall, that is, the fluid flows in the whole channel as M increases. However, vertically applied magnetic field causes the flow to concentrate in front of the left wall forming a boundary layer. Magnetic field in the $x-$direction prevents the formation of the secondary flow in front of the right part of the cavity which is observed in the case of vertical magnetic field due to the constriction. When the enclosure is constricted further, flow is squeezed through the left wall regardless of the direction of the magnetic field. For the MHD flow in the constricted enclosure, electric potential is generated and included to the MHD flow equations due to the applied magnetic field in the pipe-axis direction. Electric potential has the same behavior of the flow. As M increases, the magnitude of the velocity (flow is flattened) and electric potential decrease but the pressure increases. The increase in the constriction ratio first causes the secondary vortex of the electric potential to enlarge in the right part of the enclosure, then it concentrates through the constricted area. The numerical solutions are obtained with a considerably low computational cost through the use of radial basis function approximation.

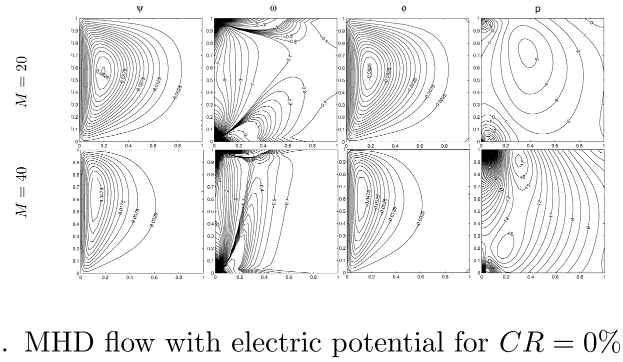

Figure 8. MHD flow with electric potential for $CR = 0\%$, $\mathbf{H_0} = (0, 0, 1)$.

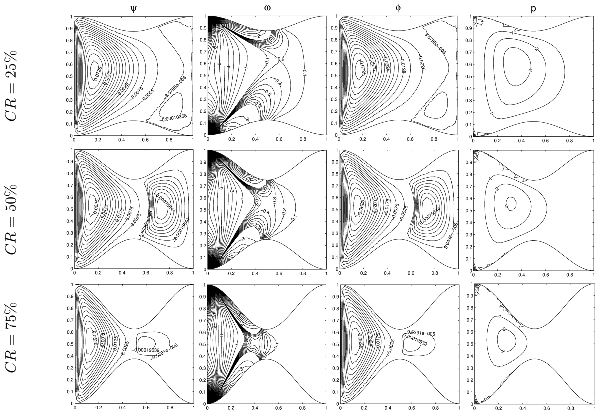

FIGURE 9. MHD flow with electric potential for $M = 20$, $\mathbf{H_0} = (0, 0, 1)$.

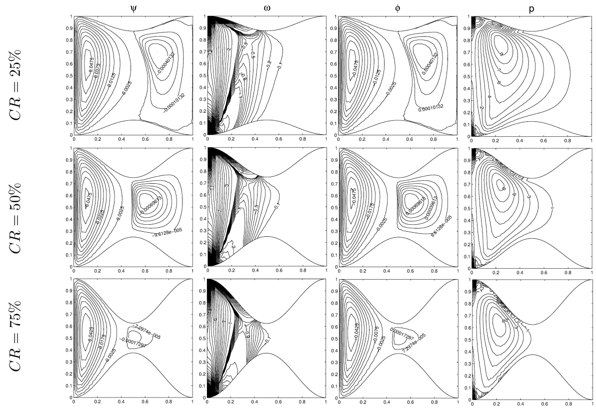

FIGURE 10. MHD flow with electric potential for $M = 40$, $\mathbf{H_0} = (0, 0, 1)$.

REFERENCES

[1] Bustamante, C.A., Power, H., Sua, Y.H. and Florez, W.F., (2013), A global meshless collocation particular solution method (integrated radial basis function) for two-dimensional Stokes flow problems, App. Math. Model, 37, pp. 4538-4547.

[2] Chen, C.S., Fan, C.M. and Wen, P.H., (2012), The method of approximate particular solutions for solving certain partial differential equations, Numer. Methods Partial Differ. Equ., 28, pp. 506-522.

[3] Eldho, T.I. and Young, D.L., (2001), Solution of Stokes flow problem using dual reciprocity boundary element method, J. Chin. Inst. Chem. Eng., 24 pp. 141-150.

[4] Galaktionav, O.S., Meleshko, V.V., Peters, G.W.M. and Meijer, H.E.H., (1999), Stokes flow in a rectangular cavity with a cylinder, Fluid Dyn. Res., 24, pp. 81-102.

[5] Gürbüz, M. and Tezer-Sezgin, M., (2015), MHD Stokes flow in lid-driven cavity and backward-facing step channel, EJCM, 24, pp. 279-301.

[6] Gürbüz, M. and Tezer-Sezgin, M., (2016), MHD Stokes flow in a smoothly constricted rectangular enclosure, Advances in Boundary Element and & Meshless Techniques XVII, 11-13 June 2016, Ankara, Turkey, pp. 73-78.

[7] Kolodziej, J.A. and Grabski, J.K., (2015), Application of the method of fundamental solutions and the radial basis functions for viscous laminar flow in wavy channel, Eng. Anal. Bound. Elem., 57, pp. 58-65.

[8] Kutanaei, S.S., Roshan, N., Vosoughi, A., Saghafi, S., Barari, A. and Soleimani, S., (2012), Numerical solution of Stokes flow in a circular cavity using mesh-free local RBF-DQ, Eng. Anal. Bound. Elem., 36, pp. 633-638.
[9] Müller, U. and Bühler, L., (2001), Magnetofluiddynamics in channels and containers, New York, Springer.
[10] Tezer-Sezgin, M. and Bozkaya, C., (2016), DRBEM solution of MHD flow and electric potential in a rectangular pipe with a moving lid, Numerical mathematics and advanced applications ENUMATH 2015, Springer, pp. 3-11.
[11] Turkyilmazoglu, M., (2010), Unsteady mhd flow with variable viscosity: Applications of spectral scheme, Int. J. Therm. Sci., 49, pp. 563-570.
[12] Turkyilmazoglu, M., (2019), MHD natural convection in saturated porous media with heat generation/absorption and thermal radiation: closed-form solutions., Arch. Mech., 71, pp. 49-64.
[13] Vasudeviah, M. and Balamurugan, K., On forced convective heat transfer for a Stokes flow in a wavy channel, Int. Commun. Heat. Mass, 28, pp. 289-297.
[14] Yosinobu, H. and Kakutani, T., (1959), Two-dimensional Stokes flow of an electrically conducting fluid in a uniform magnetic field, J. Phys. Soc. Jpn., 14, pp. 1433-1444.
[15] Young, D.L., Jane, S.J., Fan, C.M., Murugesan, K. and Tsai, C.C., (2006), The method of fundamental solutions for 2D and 3D Stokes problems, J. Comput. Phys., 211, pp. 1-8.
[16] Young, D.L., Jane, S.J., Lin, C.Y., Chiu, C.L. and Chen, K.C., (2004), Solutions of 2D and 3D Stokes laws using multiquadratics method, Eng. Anal. Bound. Elem., 28, pp. 1233-1243.
[17] Young, D.L., Tsai, C.C., Eldho, T.I. and Cheng, A.H.D., (2002), Solution of Stokes flow using an iterative DRBEM based on compactly-supported positive-definite radial basis function, CAMWA, 43, pp. 607-619.

Merve Gürbüz received her BSc and PhD degrees in mathematics from the Middle East Technical University, Turkey in 2012 and 2017, respectively. She is currently an assistant professor in the Department of Management, Başkent University, Turkey. Her research area is applied mathematics and numerical analysis.

Münevver Tezer-Sezgin received her BSc in mathematics from the Middle East Technical University, Turkey in 1974. She received her MSc and PhD degrees in Applied Mathematics in 1978 and 1980 from the University of Saskatchewan, Canada and the University of Calgary, Canada, respectively. She had one year visiting position at the University of Victoria, Canada, and short term visiting position at Technical University of Darmstadt, Germany. She is the holder of Mustafa N. Parlar 1990 Research and 2014 Science Awards in applied mathematics and engineering.